

# Dielectric and pyroelectric properties of $\text{KNO}_3$ thin-layers

F. EL-KABBANY, W. BADAUWY<sup>‡</sup>, E. H. EL-KHWAS

*Physics Department and <sup>‡</sup>Chemistry Department, Faculty of Science, Cairo University, Cairo, Egypt*

N. H. TAHR

*National Centre for Radiation Research and Technology, Cairo, Egypt*

A series of thin monocrystalline  $\text{KNO}_3$  layers has been grown from the melt by a special technique. The changes of the dielectric constant, d.c. resistivity, activation energy and pyroelectric current behaviour with the layer thickness and temperature have been investigated. Also, the effect of the a.c. frequency on the dielectric constant is checked in the frequency range 1 to 10 kHz. A sharp drop in dielectric constant could be recorded up to 6 kHz. The layers exhibit essentially the same dielectric and pyroelectric properties as bulk  $\text{KNO}_3$  single crystals. The various measured parameters of these layers were found to be thickness-dependent. The  $I$ - $V$  characteristics of the layers ( $5\ \mu\text{m}$  thickness) reveal the presence of breakdown voltage at 10.95 V. Maximum pyrocurrent was obtained at positive d.c. biasing voltage. Also, the layers show a high pyroelectric coefficient  $\gamma$ , e.g. for layer thickness  $8.9\ \mu\text{m}$ ,  $\gamma = 60\ \mu\text{C cm}^{-2}\ \text{K}^{-1}$  at  $\sim 180^\circ\text{C}$ . The study proved that thin layers of potassium nitrate have good pyroelectric properties and should be useful as pyroelectric thermal detector material.

## 1. Introduction

Various physical properties of polycrystalline and single crystals of  $\text{KNO}_3$  have been extensively studied since it is a ferroelectric material [1].  $\text{KNO}_3$  undergoes first-order phase transition from the ordered Phase II (symmetry  $D_{2h}^{16}-P_{nma}$ ) to the disordered Phase I (symmetry  $D_{6h}^3-R3C$ ) at  $135^\circ\text{C}$ . On cooling the high-temperature Phase I a metastable ferroelectric Phase III (symmetry  $C_{3v}^2-R3m$ ) appears at  $125^\circ\text{C}$  [2].

The electric properties of potassium nitrate single crystals have been studied by many authors, but nobody has dealt with the thin-layer form of this salt. Their earlier studies, however, did not throw any light on the pyroelectric properties and the nature of defects responsible for the observed conduction in this system.

Electrical measurements in thin layers of metallic nitrate single crystals and some low-symmetry crystals have nevertheless been proved to be fruitful in establishing the defect nature in corresponding crystal systems. To the best of our knowledge such measurements have not been reported in thin  $\text{KNO}_3$  layers. There are many applications of ferroelectrics which require thin layers or would be improved by the use of thin ferroelectric layers [3], for example the detection of radiation by the temperature dependence of the pyroelectric effect [4]. In fact, pyroelectric radiation detectors (PERDs) are thermal detectors with a small heat capacity due to the small thickness of the layers. The construction of a sensitive pyroelectric detector depends on the preparation of thin ferroelectric layers. The presence of good ferroelectric properties in these layers makes them promising candidates for pyroelectric radiation detector application. PERDs are unique

among the thermal radiation detectors, e.g. thermocouples, since they do not respond to a property related to their temperature  $T$ , but to its rate of temperature change  $dT/dt$ . This causes a characteristic frequency dependence of the voltage and current response of a pyroelectric detector. In the present article we report dielectric, electric and pyroelectric measurements of thin  $\text{KNO}_3$  layer single crystals prepared a special technique [5]. A series of  $\text{KNO}_3$  thin layers of different thicknesses was grown and measured.

## 2. Experimental results

### 2.1. Preparation of the single-crystal thin layers

The detailed method of preparation of the layers has been explained in our previous work [5]. In this method a suitable substrate surface is pulled out of a  $\text{KNO}_3$  melt placed in a quartz crucible [4]. In this case, a thin layer of molten  $\text{KNO}_3$  adheres to both sides of the substrate. The layer cools off above the surface of the melt and solidifies a few millimetres above the melt along a horizontal line. Therefore, the layers are highly polycrystalline at their upper end, but after about 1 cm most crystallites have disappeared; the few remaining crystallites are separated from each other by clearly visible grain boundaries. They have a general form of parallel stripes in the growth direction with a width of 1 to 2 cm. The  $\text{KNO}_3$  layers grown by this method have a suitable thickness lying between  $3.7$  and  $13.5\ \mu\text{m}$  and are smooth and flexible.

The thin layers as prepared were not transparent. There was a variation of colours from light grey to pure white depending on the layer thickness. For the

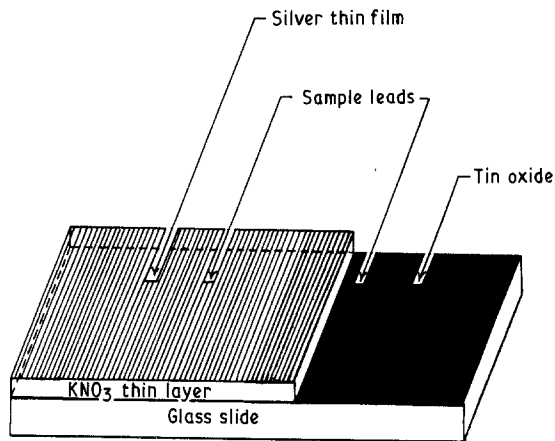
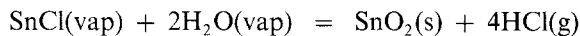


Figure 1 A sketch of a thin-layer single-crystal specimen provided with terminal electrodes.

measurements of their electric properties, the layers need contact to both sides. For this reason the substrate must be conductive to serve as one contact to the thin layer. A glass substrate coated by an  $\text{SnO}_2$  film was found to be suitable for such a function. These substrates can be obtained by the following method. Tin oxide spray was prepared in an atomizer which consists of a nozzle mounted in a 250 ml glass round-bottom flask. The water necessary for the hydrolysis reaction was supplied as vapour saturated in nitrogen. The overall reaction between  $\text{SnCl}_4$  and water at the heated substrate can be described [6, 7] by



The concentrations of  $\text{SnCl}_4$  and  $\text{H}_2\text{O}$  in the spray were adjusted with a flow-meter.  $\text{SnO}_2$  films prepared

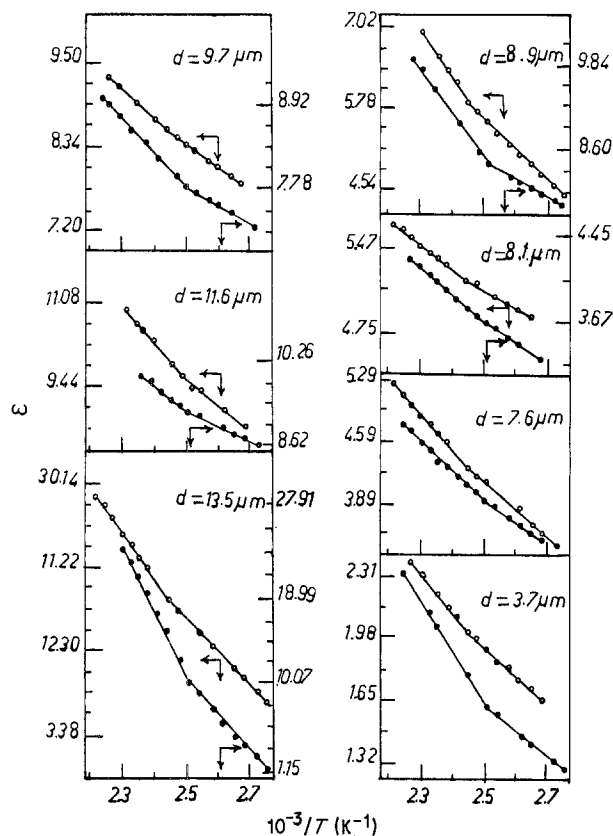


Figure 2 Variation of the dielectric constant  $\epsilon$  with  $1/T$  for different thicknesses of thin  $\text{KNO}_3$  layers: (O) heating runs, (●) cooling runs.

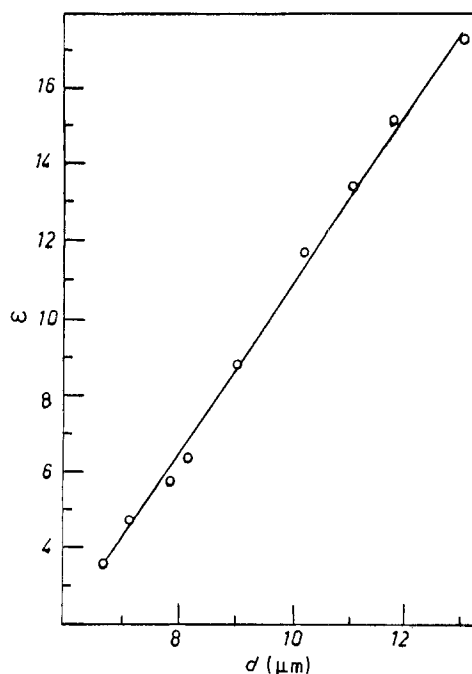


Figure 3 Variation of the dielectric constant  $\epsilon$  against the thickness  $d$  at 1 KHz.

on the glass substrate may serve as one contact. The other contact to the  $\text{KNO}_3$  layer applied after preparation of the layer may best be deposited by vacuum evaporation or by the use of silver paste. A sketch of the thin layer and its contact are shown in Fig. 1.

## 2.2. Dielectric properties

For the measurements of the dielectric properties of thin  $\text{KNO}_3$  layers, a capacitance R-L-C bridge of Heathkit type was used. It was provided with internal and external generators from 1 kHz to 1 MHz. The dielectric constant was then evaluated. All capacitors were generally stabilized before final measurements. Suitable pressure contacts and a short r.f. cable for leads were used. The variation of the dielectric constant  $\epsilon$  with the reciprocal of layer temperature  $1/T$  is shown in Fig. 2 for different layer thicknesses during heating and cooling runs. A set of linear changes are seen. The kinks observed indicates the phase transition point during heating ( $135^\circ\text{C}$ ) and during cooling ( $125^\circ\text{C}$ ). The difference in these two values is due to the well-known thermal hysteresis phenomenon [8, 9].

The effect of the layer thickness on the dielectric constant  $\epsilon$  is shown in Fig. 3. A linear change in  $\epsilon$  from 3.5 to 17 takes place as the layer thickness changed from 3.7 to  $13.5 \mu\text{m}$ . It is clear that there is a dependence of  $\epsilon$  on the layer thickness  $d$ .

The effect of frequency on the dielectric constant is shown in Fig. 4. A typical frequency-dependent nature of the dielectric constant  $\epsilon$  can be observed for layer thickness  $d \approx 5 \mu\text{m}$ . There is a sharp drop in the layer dielectric constant as the applied frequency increases to 6 kHz, followed by little change up to 10 kHz.

## 2.3. Resistivity and breakdown voltage measurements

The d.c. resistivity  $\rho_{\text{d.c.}}$  was measured for different layer thicknesses during the phase transition II  $\rightarrow$  I of

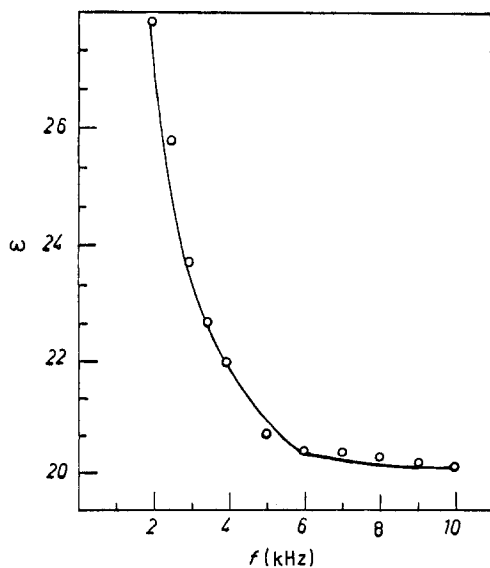


Figure 4 Variation of the dielectric constant  $\epsilon$  with the frequency  $f$ .

$\text{KNO}_3$ . The results for  $\ln \rho_{\text{d.c.}}$  are plotted as a function of  $1/T$  (Fig. 5) in order to facilitate the calculations of energy parameter values of  $\text{KNO}_3$  thin layers of different thicknesses in the range  $3.7$  to  $13.5 \mu\text{m}$ . A transition point at  $135^\circ\text{C}$  could be detected easily. The activation energies were determined for ordered and disordered phases of the various layer thicknesses. The results are given in Table I.

These energy values were calculated by the well-known resistivity-temperature exponential relation [10]. The data presented here for  $\text{KNO}_3$  thin layers appear to be of the same nature as those found in the other univalent alkali metal nitrates [11], implying that the effect is an order-disorder property of the  $\text{NO}_3^-$  ion. This means that the phase transition  $\text{II} \rightarrow \text{I}$

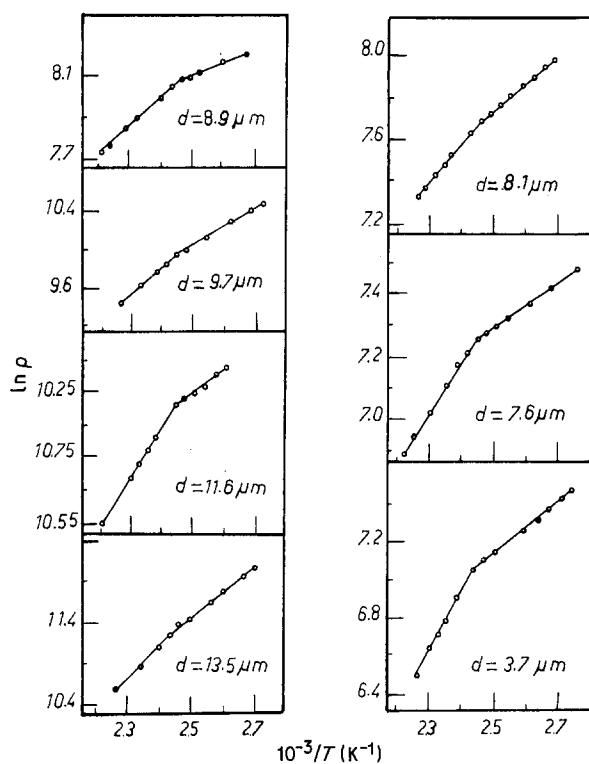


Figure 5 Variation of  $\ln \rho$  with  $1/T$  for different thicknesses of thin  $\text{KNO}_3$  layers.

TABLE I Activation energy values of Phases I and II for different layer thicknesses

Layer thickness ( $\mu\text{m}$ )	Activation energy of Phase I (eV)	Activation energy of Phase II (eV)
13.5	0.287	0.209
11.6	0.269	0.196
9.7	0.327	0.134
8.9	0.214	0.373
8.1	0.194	0.144
7.6	0.144	0.145
3.7	0.287	0.103

is a structural or order-disorder transformation. The electrical resistivity  $\rho_{\text{d.c.}}$  reflects the course of  $\epsilon$ , Fig. 2 showing that the increased polarizability is accompanied by relaxation. Although there are several accurate methods for the measurement of the breakdown voltage [12, 13], the following was adopted only for its simplicity and suitable accuracy. The layer capacitor was placed in series in a circuit consisting essentially of a d.c. source, a potential divider and a d.c. picoammeter. With a stepwise increase in voltage, the change in current was noted till there was a rapid rise in the latter with a small increase in the former. A straight line was drawn through the steeper portion of the current-voltage curves to intersect the voltage axis. This point can then be arbitrarily taken as the onset of the breakdown voltage of the capacitor. Fig. 6 shows the current-voltage characteristics of a thin  $\text{KNO}_3$  layer of  $\sim 5 \mu\text{m}$  thickness. A sudden rise in current with a slight increase of voltage was taken as the onset of breakdown voltage  $V_b$  of the thin-layer capacitor system. For this tested sample ( $\sim 5 \mu\text{m}$  thickness), the breakdown voltage is  $10.95 \text{ V}$ .

## 2.4. Pyroelectric properties

The pyroelectric current in the  $c$  direction of the thin-layer crystal was measured by a picoammeter method. The layer was first poled by d.c. biasing voltages of 20, 50 and  $100 \text{ V}$  for about half hour at  $120^\circ\text{C}$ . After the electrodes of the crystal had been short-circuited for 5 min at this temperature, the current was measured. Fig. 7 shows the temperature dependence of the pyroelectric current of thin  $\text{KNO}_3$  layers during the well-known phase transformation  $\text{II} \rightarrow \text{I}$ . In this figure, the pyroelectric current variation against  $1/T$  is studied

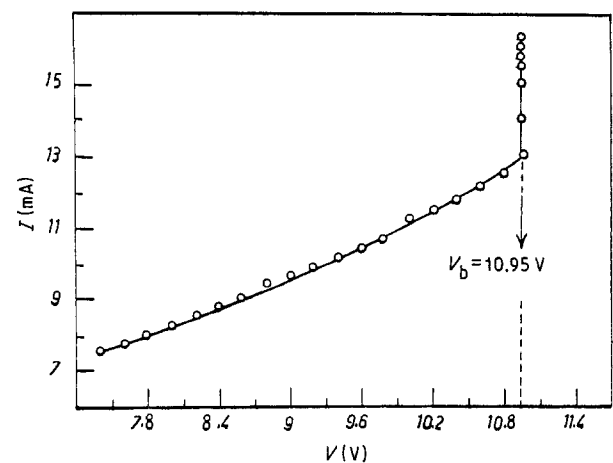


Figure 6 Current-voltage characteristic of thin  $\text{KNO}_3$  layer.

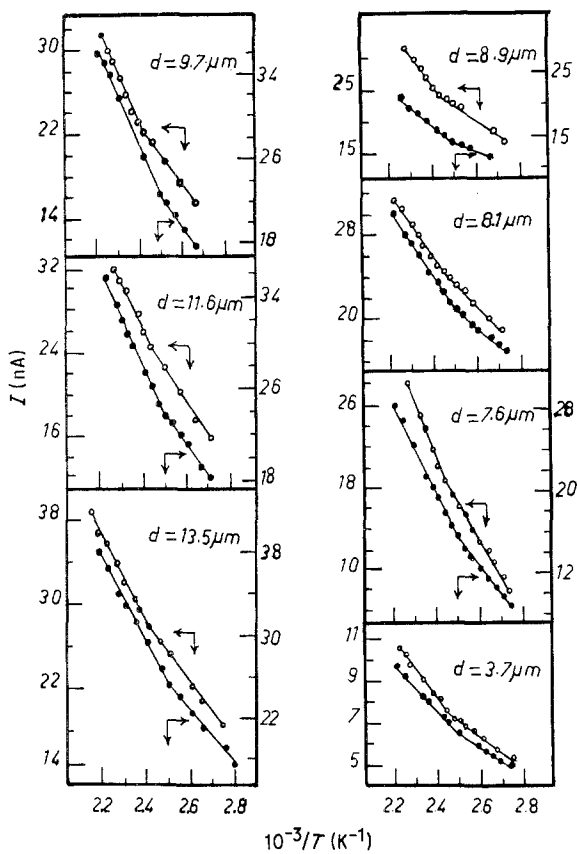


Figure 7 Variation of the pyroelectric current  $I$  with  $1/T$  for different thicknesses of thin  $\text{KNO}_3$  layers: (O) heating runs, (●) cooling runs.

for different layer thicknesses. The results agree well with the those from previous measurements. One can easily see that the pyroelectric current is dependent on layer thickness. The detailed dependence of the pyroelectric current on layer thickness is shown in Fig. 8 (upper scale). The time dependence of the pyroelectric current was also checked here (lower scale of Fig. 8) and it was found that a steady state of the current was reached after nearly 20 min whether the biasing was

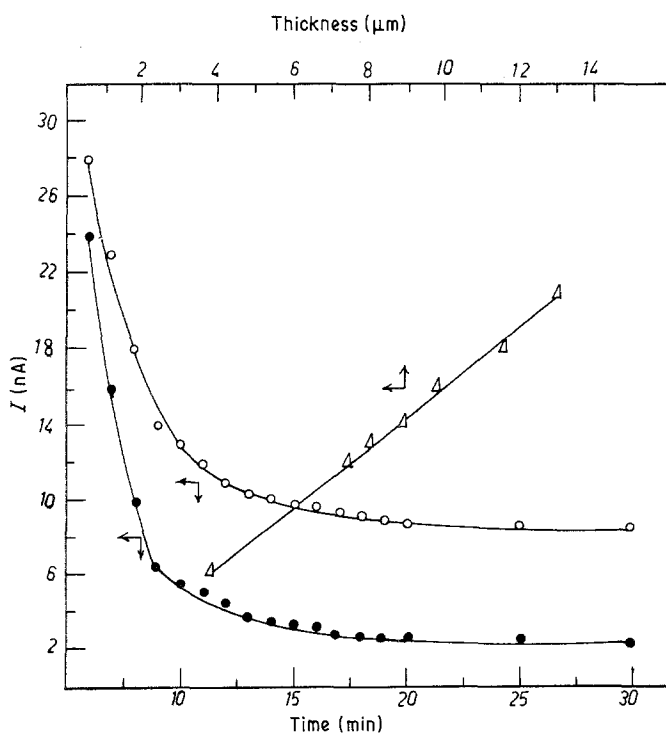


Figure 8 Variation of the pyroelectric current  $I$  with layer thickness and time under (O) +50 V, (●) -50 V and (Δ) zero biasing voltage.

positive or negative. Also the effect of d.c. biasing on the pyroelectric current of the layer was tested for positive voltages of 20, 50 and 100 V and negative voltages -20, -50 and -100 V. The results are shown in Fig. 9, which shows that the maximum pyroelectric current will be obtained for maximum positive biasing voltage.

### 3. Discussion

The results obtained in the present work on thin layers confirm the previous findings of single-crystal and polycrystalline measurements that  $\text{KNO}_3$  undergoes a high-temperature phase transition  $\text{II} \rightarrow \text{I}$  at  $135^\circ\text{C}$ . Although this is not one of the fundamental goals of this work, it is the first impression one can obtain. The observed increase in the dielectric constant and decrease in d.c. resistivity associated with the phase transition  $\text{II} \rightarrow \text{I}$  implies the possible existence of some order-disorder mechanism responsible for the observed transition. The high values of  $\gamma$  obtained from these two phases I and II imply that lattice dipoles could become relatively easily distorted or rotated in these two phases, and hence exceptionally large amplitudes might result from the presence of positional or rotational disorder in the lattice. The observed linear increase in  $\gamma$  with increase of temperature is widely accepted for ionic dielectrics. The dielectric features of  $\text{KNO}_3$  thin layers may be understood from the following considerations.

The a.c. characteristics of thin-layer dielectrics can broadly be explained utilizing two types of theoretical model:

- (i) a single capacity element with appropriate resistances in series and parallel as proposed by Goswami and Goswami [14];
- (ii) three capacity elements arising from two additional barrier layers with appropriate parallel resistance as proposed by Simmons and co-workers [15, 16].

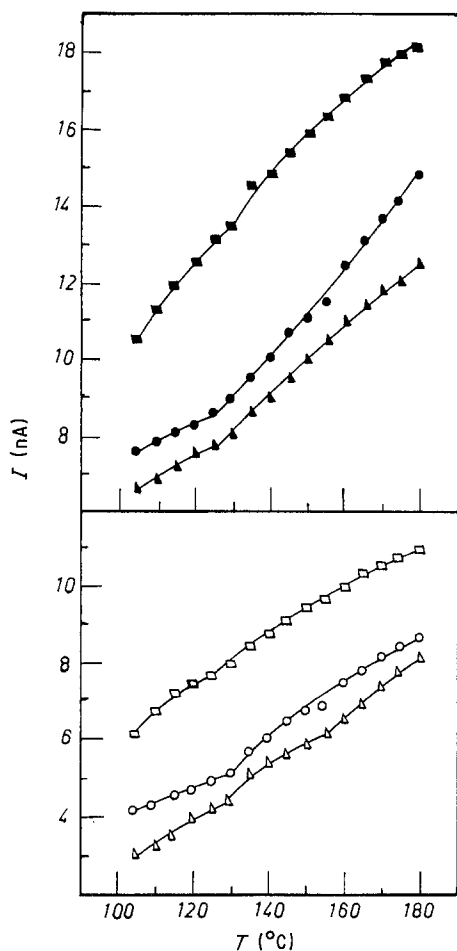


Figure 9 Variation of the pyroelectric current  $I$  with temperature  $T$  under different biasing voltages: (■) +100 V, (●) +50 V, (▲) +20 V; (□) -100 V, (○) -50 V, (△) -20 V.

The dielectric constant behaviour of the  $\text{KNO}_3$  layers studied here agrees with only one of the above two models. The thickness dependence of dielectric constant throughout the layer thickness range seems to be in accordance with the barrier-layer model [2]. It seems reasonable to imagine that the steep reduction of the electrical resistivity of a  $\text{KNO}_3$  layer at the transition point ( $135^\circ\text{C}$ ) corresponds to the appearance of some disordering in the position or orientation of the atoms or radicals, which is related in some degree at least with the free rotation of  $\text{NO}_3$  groups at high temperature. It is known that the  $\text{NO}_3$  group is able to rotate in the crystal under appropriate conditions. For instance, the transition point ( $275^\circ\text{C}$ ) just below the melting point ( $310^\circ\text{C}$ ) of  $\text{NaNO}_3$  is generally considered to be a temperature at which  $\text{NO}_3$  groups begin to rotate almost freely. Hence it would not be unreasonable to imagine that, also in the high temperature Phase I of  $\text{KNO}_3$ ,  $\text{NO}_3$  groups are more or less making rotations about the  $c$ -axis. In the ordered Phase II, on the other hand,  $\text{NO}_3$  groups are considered to be fixed in definite orientations in the  $c$  plane and accordingly in definite positions along the  $c$  axis.

The electric conduction process in  $\text{KNO}_3$  is evidently [17] ionic and could thus occur either via jumps or through interstitial jumps of  $\text{K}^+$  ions.

It seems reasonable to assume that at all temperatures investigated, the electrical conductance is

due to the movements of  $\text{K}^+$  ions. At relatively low temperature these ions probably move through the lattice in interstitial positions and along dislocations. It might be expected, therefore, that an increase in specific volume would increase the mobility of defect ions and hence the measured conductance. According to Rao and Rao [18], the phase transition  $\text{II} \rightarrow \text{I}$  of  $\text{KNO}_3$  is accompanied by an increase in molar volume by  $0.83 \text{ cm}^3 \text{ mol}^{-1}$ . In the present measurements, the conductance increases approximately tenfold after the phase transformation. The question then arises whether the increase in conductance is due to an increase in defect ion mobility or due to an increase in the number of mobile ions.

In Phase II, the  $\text{NO}_3^-$  ions are partly orientationally disordered and this involves the rupturing of O-K bonds. This might be expected to increase the probability of a  $\text{K}^+$  ion moving away from its lattice site. On the other hand, a reorienting  $\text{NO}_3^-$  ion would occupy a greater volume than a fixed one, and this would tend to decrease the interstitial space.

The pyroelectricity [19] which arises here can probably be attributed to the high electric fields which develop across insulating pyroelectrics subjected to relatively small temperature changes. At equilibrium the depolarization fields due to the polarization discontinuity at the surface of the thin-layer pyroelectric crystal are neutralized by free charge. When the layer temperature is changed the spontaneous polarization changes, so that an excess of free charge appears on one of the polar planes which gives rise to current flow in the layer and external circuit. The sense of the pyrocurrent depends on the direction of polarization change.

The pyroelectric coefficient was calculated here using the relation [20]

$$\gamma = I \left( \frac{dT}{dt} \right)^{-1} / S$$

where  $I$  is the current,  $S$  is the area of the specimen and  $dT/dt$  is the rate of heating. The pyroelectric coefficient deduced from the present results is shown as a function of temperature in Fig. 10. Its value at room temperature agrees well with that observed for bulk crystals. According to the present work, one can say that thin layers of  $\text{KNO}_3$  appear to be well suited to a pyroelectric radiation detector material. The pyroelectric coefficient  $\gamma$  at room temperature is not as high as (for example) in triglycine sulphate, because the Curie point  $T_c$  is higher for  $\text{KNO}_3$  than for triglycine sulphate [21]. A high  $T_c$  value is basically an advantage, since partial depolarization near  $T_c$  leads to the destruction of the spontaneous polarization. As shown,  $\text{KNO}_3$  may readily be prepared in thin layers of various thickness possessing nearly the same properties. This gives more control for the construction of PERDs with small heat capacity. The heat capacity of the pyroelectric sensors should be as small as possible to allow large temperature changes for a given amount of radiation energy. Thus  $\text{KNO}_3$  thin layers can be considered as good pyroelectric material and should be useful in a pyroelectric thermal detector.

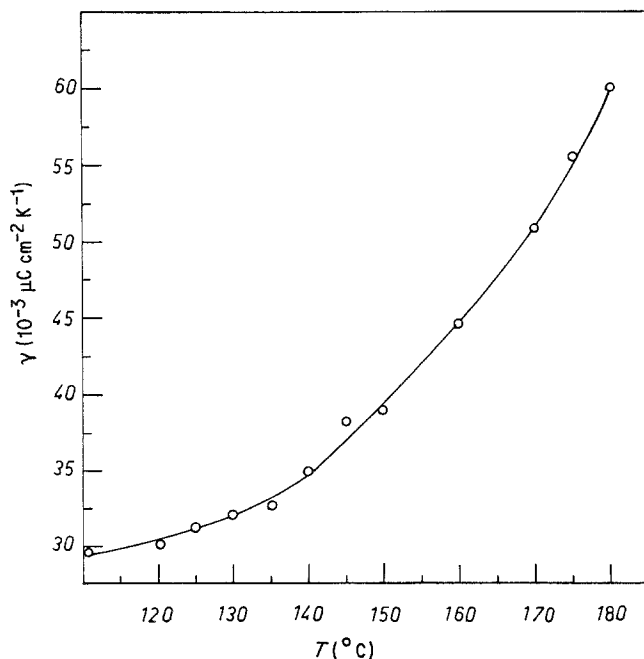


Figure 10 Variation of the pyroelectric coefficient  $\gamma$  with the layer temperature  $T$ . Layer thickness  $8.9 \mu\text{m}$ .

## References

1. S. SAWADA, S. NOMURA and Y. ASAO, *J. Phys. Soc. Jpn* **16** (1961) 12.
2. P. E. TAHVONEN, *Ann. Acad. Sci. Fennicae Ser. A* **1** (1947) 44.
3. XU YUHUAU, C. HUOCHU and L. E. CROSS, *Ferroelec. Lett.* **2** (1984) 189.
4. H. VOGT, P. WURFEL, U. HETZLER and W. RUPPEL, *Ferroelectrics* **33** (1981) 243.
5. T. HAMMAD, F. EL-KABBANY and Y. BADR, *Phys. Status Solidi (a)* **94** (1986) 121.
6. R. N. GHOSHTAGOR, in Proceedings of International Conference on Chemical Vapour Deposition VI, Princeton, p. 433; *Proc. Electron. Soc. (USA, 1977)* 77-5.
7. W. BADAUWY, F. DECKER and K. DOBLHOFER, *Solar Energy Mater.* **8** (1983) 363.
8. F. EL-KABBANY, Y. BADV, G. SAID, S. TAHA and S. MAHROUS, *Phys. Status Solidi (a)* **95** (1986) 127.
9. F. EL-KABBANY, *ibid.* **58** (1980) 373.
10. *Idem*, *Appl. Phys. Commun.* **6** (1) (1986) 57.
11. F. EL-KABBANY, G. SAID, S. MAHROUS and S. TAHA, *Phys. Status Solidi (a)* **95** (1986) 495.
12. P. P. BUDEUSTEIN and P. J. HAYES, *Appl. Phys.* **38** (1967) 2837.
13. F. FORLANT and N. MINNAJA, *J. Vac. Sci. Techn.* **6** (1969) 518.
14. A. GOSWAMI and A. P. GOSWAMI, *Thin Solid Films* **16** (1973) 175.
15. J. G. SIMMONS, G. S. NADARNI and M. C. LANCASTER, *J. Appl. Phys.* **41** (1970) 538.
16. G. S. NADARNI and J. G. SIMMONS, *ibid.* **41** (1970) 545.
17. J. P. NOLTA, N. W. SCHUBRING and R. A. DORK, *J. Chem. Phys.* **42** (1965) 508.
18. K. J. RAO and C. N. R. RAO, *J. Mater. Sci.* **1** (1966) 238.
19. S. B. LANG, "Source book of Pyroelectricity" (Gordon and Breach, New York, 1974) p. 238.
20. M. E. LINES and A. M. GLASS, "Principles and Applications of Ferroelectrics and Related Materials" (J. W. Arrowsmith, Bristol, 1977).
21. V. M. RUDYAK and BAGOMOLOV, *Ferroelectrics* **33** (1981) 25.

Received 23 December 1986  
and accepted 27 April 1987